



**Fermilab**

TM-1416  
0102.000  
(SSC-N-232)

**COMMENTS ON THE IMPEDANCES OF THE  
SSC SHIELDED BELLOWS AT LOW FREQUENCIES  
DUE TO THE TRUNCATION OF THE WAKE FIELDS**

K.-Y. Ng

September 1986

(Submitted to the Proceedings of the 1986 Summer Study on the Physics of the Superconducting Super Collider, Snowmass, Colorado, June 23-July 11, 1986)

# COMMENTS ON THE IMPEDANCES OF THE SSC SHIELDED BELLOWS AT LOW FREQUENCIES DUE TO THE TRUNCATION OF THE WAKE POTENTIALS

K. Y. Ng

Fermi National Accelerator Laboratory\*, Batavia, IL 60510

## ABSTRACT

The behavior of the longitudinal impedance of the SSC shielded bellow at low frequencies depends very much on the length of the wake field used in the Fourier transformation. We show analytically and numerically that, regardless of the difference, single-bunch effects are independent of the actual shape of the impedance when the length of the wake used is bigger than the bunch length.

## INTRODUCTION

The SSC bellows are shielded as in Fig. 1 in order to reduce impedances. Both the longitudinal and transverse impedances of such a system have been computed<sup>1,2</sup> and are reviewed in the Conceptual Design Report<sup>3</sup>. In particular, the real part of the longitudinal impedance is shown in Fig. 2a. We see that, at low frequencies, the impedance is  $6.67 \Omega$ . This can be understood by the fact that electromagnetic energy is leaking through the gap, which can be viewed as a coaxial transmission line of inner and outer radii 1.7 and 1.9 cm connected in parallel to the beam pipe. Thus, the impedance is just  $Z_c = (Z_0/2\pi)\ln(1.9/1.7) = 6.67 \Omega$ , the characteristic impedance of the transmission line,  $Z_0 = 377 \Omega$  being the free-space impedance. At the Snowmass Workshop, it was pointed out that such an impedance plot cannot be correct since the feeding of energy into the shielded part of the bellow system cannot continue for ever. When equilibrium is reached, flow of energy is no longer possible. In other words, the longitudinal impedance at low frequencies should be zero instead. It is the purpose of this paper to investigate this problem. Our result shows that the latter picture is indeed correct. However, for the purpose of studying single-bunch properties such as instabilities and parasitic losses, the impedance plot of Fig. 2 will lead to the correct results and is simpler also.

## THE MONOPOLE MODE

We compute the longitudinal wake field of the

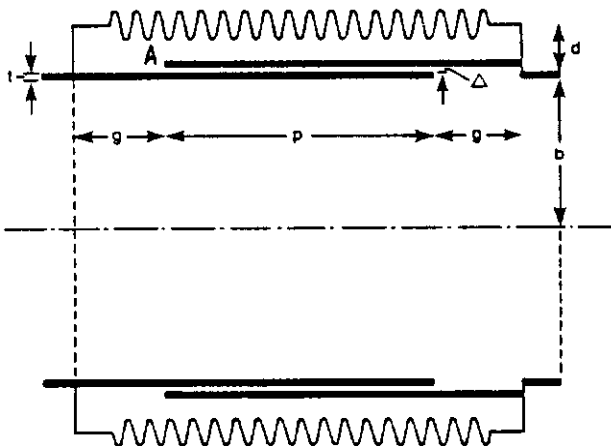


Fig. 1. The shielded bellow.  $p = 30$  cm,  $g = 10$  cm,  $b = 1.5$  cm,  $d = 9$  mm,  $t = \Delta = 2$  mm.

\*Operated by the Universities Research Association, under contract with the U.S. Department of Energy.

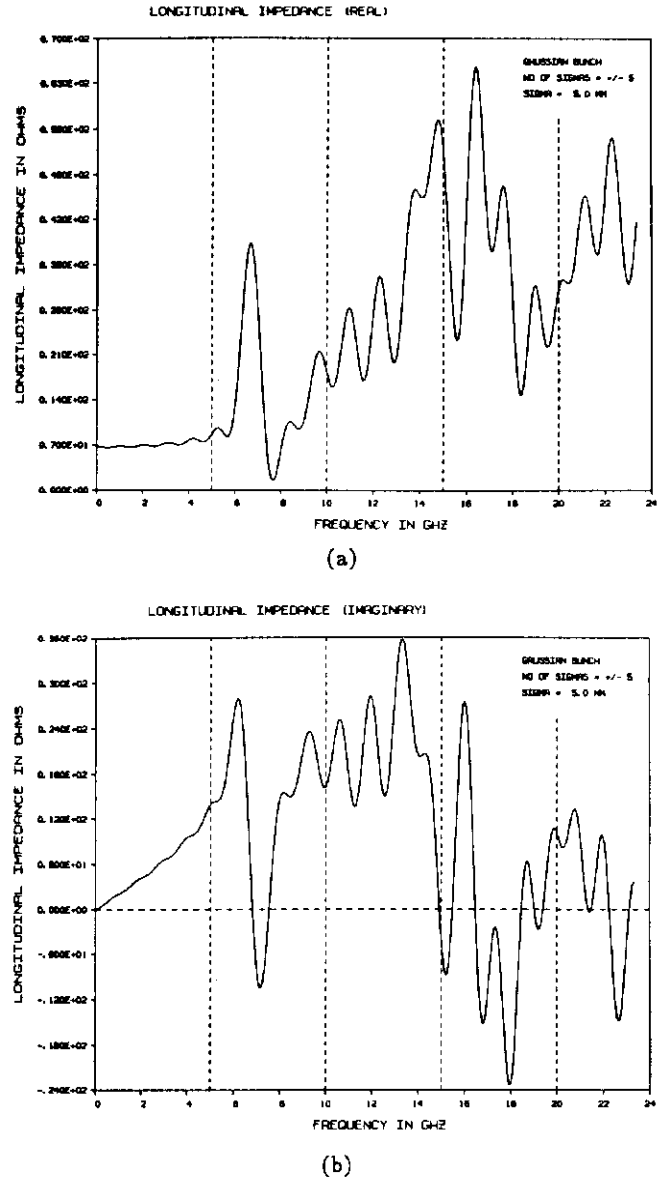


Fig. 2. (a) real and (b) imaginary parts of  $Z_L$  computed from only 30 cm of the wake potential in Fig. 3.

configuration in Fig. 1 up to a length of 4.096 m with a mesh size of 0.5 mm. The result is shown in Fig. 3. The real and imaginary parts of the Fourier transform give the longitudinal impedance and are displayed in Fig. 4. We see that the structure of the impedance is totally different from that in Fig. 1 where only 30 cm of the wake is used. In Fig. 4, we do not see  $6.67 \Omega$  at low frequencies indicating the fact that energy is not being fed into the shielded cavity indefinitely. The exact value at zero frequency is not known; its determination requires the wake up to infinity. We see many sharp resonances at nearly every half GHz which correspond to wave bouncing back and forth in the 30 cm overlapping region of the sliding shields. In fact, such reflection for roughly every 60 cm can be seen in the wake potential in Fig. 3. The reason for the appearance of the first resonance at near zero

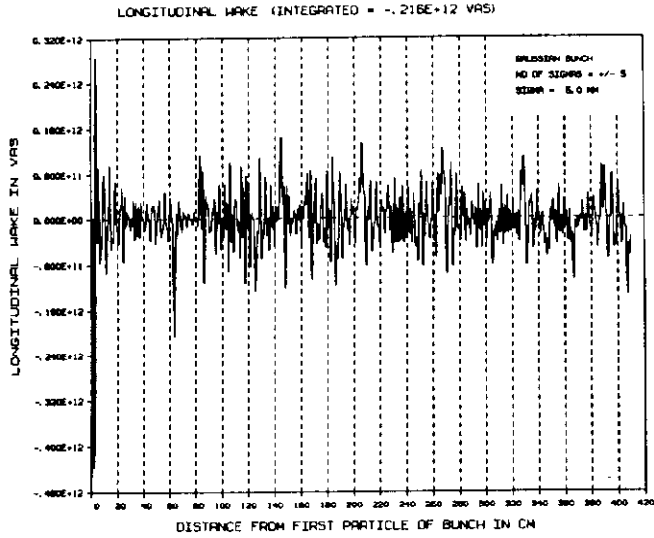


Fig. 3. Longitudinal wake potential of shielded bellow.

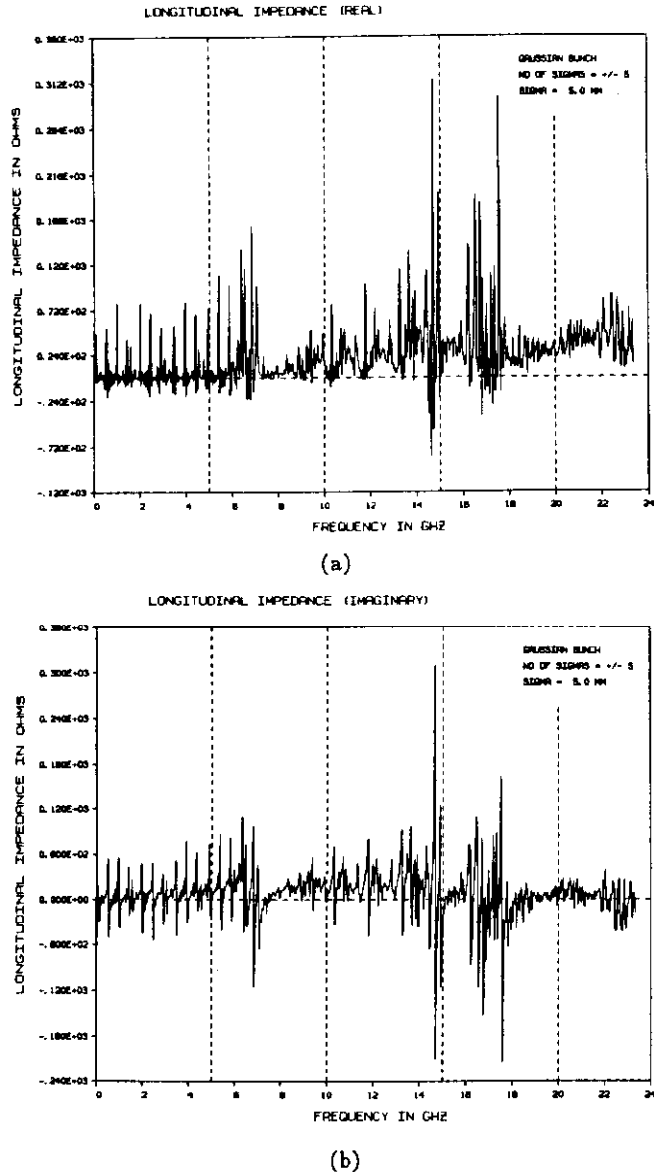


Fig. 4. (a) real and (b) imaginary parts of  $Z_L$  computed with ~4.1 m of wake potential in Fig. 3.

frequency is unknown.

We know that many physical phenomena such as single-bunch-mode instabilities and parasitic energy loss depend only on the low-frequency part of the impedance where the amplitude of the bunch spectrum is not too small. However, the low-frequency parts of Figs. 2 and 4 are so much different; how can they produce the same result? The answer lies in the fact that the SSC bunch has an RMS length of only  $\sigma = 7$  cm. The interactions between the particles inside the bunch only depend on ~30 cm of the wake potential. So both Figs. 2 and 4 should lead to the same single-bunch effects. Physically speaking, the bunch, because of its short length, will not be able to see the wave it sends out to bounce back from the overlapping region of the sliding shields. In other words, for single-bunch effects, the structure in Fig. 1 can be simplified by closing the end A of the overlapped shields.

To demonstrate the equivalence of Figs. 2 and 4 for single-bunch effects, let us compute the rate of parasitic loss of an SSC bunch passing through a shielded bellow structure. This rate of loss is given by

$$\frac{d\epsilon}{dt} = c \int_{-\infty}^{+\infty} dz \int_{-\infty}^z dz' \rho(z) \rho(z') W_L(z-z'), \quad (1)$$

where  $c$  is the velocity of light,  $W_L$  the longitudinal wake potential and

$$\rho(z) = \frac{eN}{\sqrt{2\pi}\sigma} \exp[-z^2/2\sigma^2] \quad (2)$$

is the linear bunch density carrying a total charge of  $eN$ . The upper integration limit of  $z'$  in Eq. (1) can be extended from  $z$  to  $+\infty$  because of the causality property of  $W_L$ . But, in reality, because of Eq. (2), the integration ranges of both  $z$  and  $z'$  are only approximately from  $-2\sigma$  to  $+2\sigma$ . As a result, only about 40 or a length equal to the approximate length of the bunch is needed for the wake.

In the frequency domain, we can write

$$\rho(z) = \sum_p \rho_p \exp[-jp\omega_0 z/c], \quad (3)$$

$$W_L(z) = \frac{\omega}{2\pi} \sum_p Z_L(p\omega_0) \exp[jp\omega_0 z/c], \quad (4)$$

with

$$\rho_p = \frac{eN\omega_0}{2\pi c} \exp\left[-\frac{1}{2}\left(\frac{p\omega_0\sigma}{c}\right)^2\right], \quad (5)$$

$\omega_0$  the angular revolution frequency of the accelerator ring, and  $Z_L$  is the longitudinal impedance. In Eqs. 3 and 4, the summations are for all integers  $p$  from  $-\infty$  to  $+\infty$ . Then, the rate of parasitic loss becomes

$$\frac{d\epsilon}{dt} = \frac{(eN\omega_0)^2}{4\pi^2} \sum_p Z_L(p\omega_0) \exp[-(p\omega_0\sigma/c)^2]. \quad (6)$$

Because the circumference of the SSC ring is so much bigger than the bunch length, the summation over  $p$  can be transformed into an integral; or

$$\frac{d\epsilon}{dt} = \frac{(eN)^2 \omega_0}{2\pi} L_n, \quad (7)$$

where the integral  $L_n$  is defined as

$$L_n = \frac{1}{2\pi} \int_{-\infty}^{+\infty} (\omega/2\pi)^n Z_L(\omega) \exp[-(\omega\sigma/c)^2] d\omega, \quad (8)$$

which is independent of the size of the ring. We want to examine this general integral because it will appear in various single-bunch effects; for example, frequency shifts and growth rates of various single-bunch mode oscillations. This integral will result when differentiation of order  $n$  is performed on the wake potential in Fig. 1. As a result, this integral should also be independent of the length of the wake from which  $Z_L$  is derived as long as the length is larger than the bunch length. Note that only the real (imaginary) part of  $Z_L$  will contribute if  $n$  is even (odd). This integral is computed with the  $Z_L$  of Fig. 2 and also that of Fig. 4; the results are listed in Table I.

	Fig. 2	Fig. 4	Eq. (12)
$L_0$ ( $\Omega/\text{ns}$ )	8.068	8.067	8.07
$L_1$ ( $\Omega/\text{ns}^2$ )	j0.566	j0.566	j0.59
$L_2$ ( $\Omega/\text{ns}^3$ )	1.877	1.879	1.88
$L_3$ ( $\Omega/\text{ns}^4$ )	j0.398	j0.396	j0.41
$L_4$ ( $\Omega/\text{ns}^5$ )	1.315	1.313	1.31
$L_5$ ( $\Omega/\text{ns}^6$ )	j0.460	j0.461	j0.48

Table I

Table I obviously demonstrates that the integral  $L_n$  is indeed independent of whether Fig. 2 or Fig. 4 is used for the impedance. In fact, Fig. 2 is a lot simpler because at low frequencies over the spectral range of the bunch,  $\text{Re}(Z_L)$  and  $\text{Im}(Z_L/\omega)$  are almost constant and can be derived. As is shown above, at low frequencies,

$$\text{Re}(Z_L) = \frac{Z_0 g_a}{2\pi} \ln \frac{r_2}{r_1} \sim \frac{Z_0 \Delta}{2\pi r_1} \quad (9)$$

is the characteristic impedance of the transmission line formed by the overlapping shields of inner and outer radii  $r_1$  and  $r_2$  respectively and gap size  $\Delta = r_2 - r_1$ . The cavity to the right of the overlapping shields can also be considered<sup>4</sup> as a transmission line connected in series with the beam pipe of radius  $r_0$  ( $= 1.5$  cm). At low frequencies, the impedance is

$$\frac{Z_L}{\omega} = j \frac{Z_0 g_a}{2\pi c} \ln \frac{r_2}{r_0} \sim j \frac{Z_0 g_a \Delta'}{2\pi r_0}, \quad (10)$$

where  $\Delta' = r_2 - r_0$  and  $g_a$  is the effective attenuated line length (since propagation is impossible below cutoff) relating to the actual length  $g$  ( $= 10$  cm) by

$$g_a = \frac{1 - e^{-\gamma g}}{\gamma} \quad (11)$$

with  $\gamma = 2.405/r_2$ . We get  $\text{Im}(Z_L/\omega) = 0.374 \Omega\text{-ns}$  in agreement with the initial slope of  $0.329 \Omega\text{-ns}$  in Fig. 2b. Then, the integral  $L_n$  can be performed analytically by taking the impedance outside the integration sign, giving

$$L_n = \begin{cases} \text{Re}(Z_L) \left(\frac{c}{2\pi\sigma}\right)^{n+1} \Gamma\left(\frac{n+1}{2}\right) & n \text{ even} \\ 2\pi \text{Im}\left(\frac{Z_L}{\omega}\right) \left(\frac{c}{2\pi\sigma}\right)^{n+2} \Gamma\left(\frac{n+2}{2}\right) & n \text{ odd} \end{cases} \quad (12)$$

where the impedance is given approximately by Eqs. (9) and (10). The evaluation of Eq. (12) is listed in the last column of Table I for comparison. The advantage of using a short wake or the impedance shown in Fig. 2 is obvious. Here, Eq. (12) can tell us how the parasitic loss as well as other quantities of interest are dependent on the various parameters of the shielded bellow system. For example, the parasitic loss is approximately proportional to the gap  $\Delta$  of the sliding shields when  $\Delta \ll r_1$ . On the other hand, the more exact impedance in Fig. 4 tells us nothing. In our situation, for  $M = 17280$  bunches each containing  $N = 7.3 \times 10^9$  protons and  $\sim 5000$  such shielded bellow systems, the rate of parasitic loss is  $\sim 3500$  watts. In the Conceptual Design Report<sup>4</sup>, they take  $r_1 = 1.65$  cm and find that, in order to reduce this loss to an acceptable one of  $\sim 190$  watts, the sliding gap  $\Delta$  cannot exceed  $0.1$  mm. Our formula agrees with such a conclusion, although a sliding gap of such small size is not practical in reality. An easier solution is to place fingers closely along the circumference of the gap so that no radiation of low frequencies can penetrate.

### DIPOLE MODE

We now consider the transverse mode. The transverse wake  $W_T$  (Fig. 5) is computed up to a length of  $2.6$  m. A longer wake is impossible because TBCI starts to diverge after such length in the dipole mode. The transverse impedance  $Z_T$  is defined by

$$W_T(z) = -j \frac{\omega}{2\pi} \sum_p Z_T(p\omega_0) \exp[jp\omega_0 z/c], \quad (13)$$

and is plotted in Fig. 6 computed using only  $30$  cm of wake and Fig. 7 using the whole wake available. Unlike the longitudinal case, here the plots are similar although the resolution is much higher in Fig. 7.

We can also compute a similar integral  $T_n$  for the transverse mode:

$$T_n = \frac{1}{2\pi} \int_{-\infty}^{+\infty} (\omega/2\pi)^n Z_T(\omega) \exp[-(\omega\sigma/c)^2] d\omega. \quad (14)$$

Here, only the imaginary (real part) of  $Z_T$  will contribute when  $n$  is even (odd). The numerical results are listed in Table II.

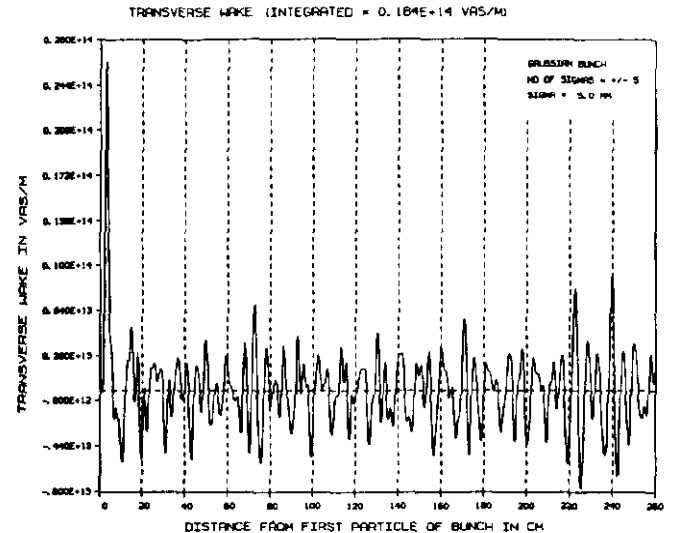
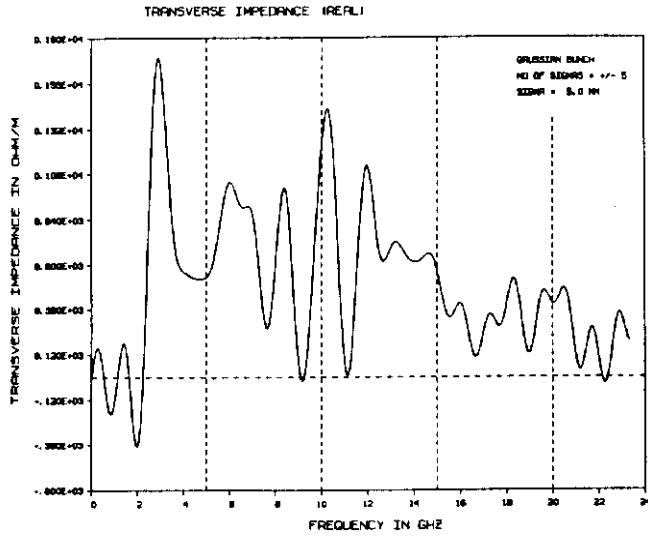
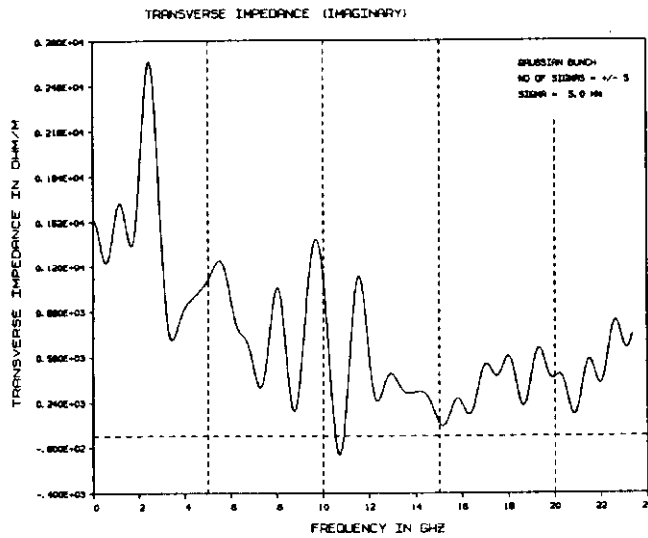


Fig. 5. Transverse wake potential of shielded bellow.



(a)



(b)

Fig. 6. (a) real and (b) imaginary parts of  $Z_T$  computed from only 30 cm of wake potential in Fig. 5.

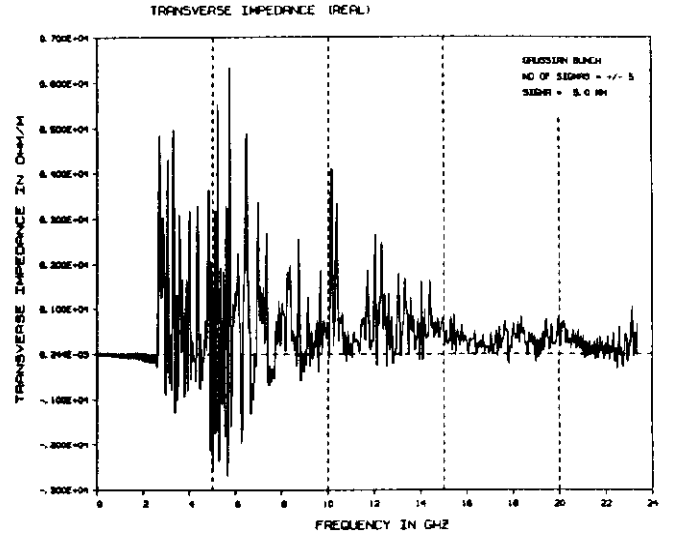
Fig. 6

Fig. 7

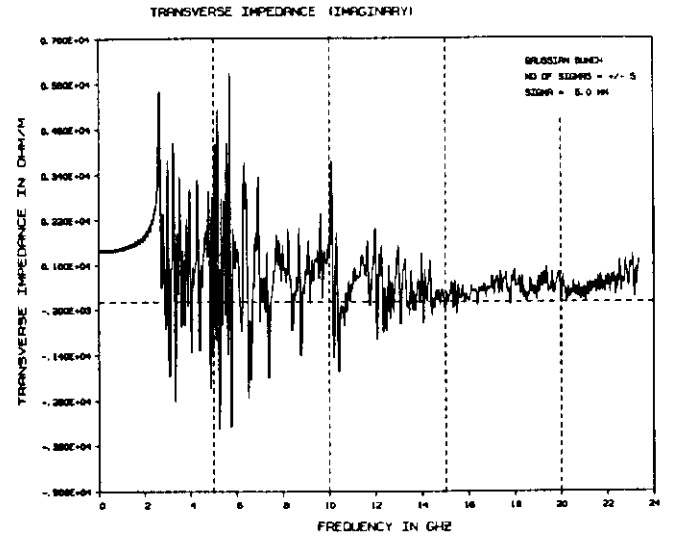
$T_0$ ( $\Omega/\text{m}\cdot\text{ns}$ )	j0.169E+4	j0.168E+4
$T_1$ ( $\Omega/\text{m}\cdot\text{ns}^2$ )	-0.231E+0	-0.630E+0
$T_2$ ( $\Omega/\text{m}\cdot\text{ns}^3$ )	j0.393E+3	j0.399E+3
$T_3$ ( $\Omega/\text{m}\cdot\text{ns}^4$ )	-0.111E+2	-0.488E+2
$T_4$ ( $\Omega/\text{m}\cdot\text{ns}^5$ )	j0.289E+3	j0.285E+3
$T_5$ ( $\Omega/\text{m}\cdot\text{ns}^6$ )	-0.604E+1	-0.530E+1

Table II

We see that, when  $n$  is even,  $T_n$  is independent of the length of wake used so long if it is longer than the length of the bunch. However, when  $n$  is odd, the values of  $T_n$  differ. If we use a slightly longer wake,



(a)



(b)

Fig. 7. (a) real and (b) imaginary parts of  $Z_T$  computed from the 2.6 m of the wake potential in Fig. 5.

for example, 40 cm, good agreement is obtained. As given by Eq. (14),  $T_n$  should be positive when  $n$  is odd since  $\text{Re}[Z_T(\omega)]$  cannot be negative for positive frequency  $\omega$ . On the other hand at low frequencies  $\text{Re}[Z_T]$  is identically zero so that  $T_n$  should be very small for odd  $n$ . Our results are small but unfortunately negative. This may be due to the inaccuracy of TBCL in computing the wake field. Since  $\text{Im}[Z_T]$  is constant at low frequencies, a formula similar to Eq. (12) can be derived for  $T_n$  when  $n$  is even.

#### REFERENCES

1. K. L. F. Bane and R. D. Ruth, Proceedings of the SSC Impedance Workshop, Berkeley, 1985.
2. K. Y. Ng, Proceedings of the SSC Impedance Workshop, Berkeley, 1985.
3. Conceptual Design of the SSC, Edited by J. D. Jackson, 1986.
4. M. Furman, SSC Design Group Internal Report No. SSC-N-142 (1986).